

Neural Grasp Distance Fields for Robot Manipulation

Thomas Weng^{1,2}, David Held², Franziska Meier¹, and Mustafa Mukadam¹

¹Meta AI, ²Carnegie Mellon University

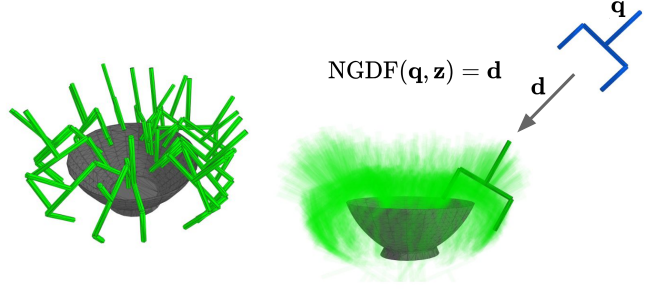
Abstract— We formulate grasp learning as a neural field and present Neural Grasp Distance Fields (NGDF). Here, the input is a 6D pose of a robot end effector and output is a distance to a continuous manifold of valid grasps for an object. In contrast to current approaches that predict a set of discrete candidate grasps, the distance-based NGDF representation is easily interpreted as a cost, and minimizing this cost produces a successful grasp pose. This grasp distance cost can be incorporated directly into a trajectory optimizer for joint optimization with other costs such as trajectory smoothness and collision avoidance. During optimization, as the various costs are balanced and minimized, the grasp target is allowed to smoothly vary, as the learned grasp field is continuous. In simulation benchmarks with a Franka arm, we find that joint grasping and planning with NGDF outperforms baselines by 63% execution success while generalizing to unseen query poses and unseen object shapes. Project page: <https://sites.google.com/view/neural-grasp-distance-fields>.

I. INTRODUCTION

We present *Neural Grasp Distance Fields* (NGDF), which model the continuous manifold of valid grasp poses as the level set of a neural implicit function. Given a 6D query pose, NGDF predicts the unsigned distance between the query and the closest valid grasp on the manifold (see Fig. 1).

Neural implicit fields have driven recent advancements in novel view synthesis [1] and 3D reconstruction [2], [3], [4], [5]. These approaches represent distributions as continuous functions that take a query as input and predict its relationship to the learned distribution. In 3D shape reconstruction, for instance, neural implicit fields are used to represent the surface of a shape: 3D points are used as queries, and the output is the distance to the surface, or occupancy at the query point. Unlike explicit methods, neural implicit fields can encode complex topological distributions and are not limited by resolution.

With NGDF, formulating grasp learning as a neural field allows us to interpret the implicit function as a cost such that a query pose can be optimized to result in a grasp pose. Prior grasp estimation methods largely output a discrete set of candidate grasps [6], [7], [8], [9], [10], from which one grasp must be selected to perform downstream planning. Instead, we incorporate the grasp distance cost directly into a gradient-based optimizer [11] to jointly optimize the grasp and reaching motion from an initial trajectory. During each optimization iteration, NGDF estimates the distance between the final gripper pose of the trajectory and the grasp level set. This “grasp distance” is minimized as a cost, along with other trajectory costs such as smoothness and collision avoidance. The gradient of the grasp cost for updating the trajectory is computed through fully differentiable operations. This



(a) Discrete Grasp Set (b) Continuous Grasp Manifold with NGDF

Fig. 1: (a) Existing grasp estimation methods produce discrete grasp sets which do not represent the true continuous manifold of possible grasps. (b) Our work, Neural Grasp Distance Fields (NGDF), learns a continuous grasp manifold: given a query pose q and an object shape embedding z , NGDF outputs the distance d between q and the closest grasp. This distance can be leveraged as a cost for optimization, facilitating joint grasp and motion planning.

optimization results in a smooth, collision-free trajectory that reaches a valid grasp pose.

In experiments we find that NGDF successfully learns the level set of valid grasp poses, and generalizes to both unseen query poses and unseen object shapes. We evaluate NGDF on a level set optimization task and a reaching and grasping task, where the model provides the grasp distance cost that a trajectory optimizer jointly optimizes with other trajectory costs. We outperform existing methods that use predicted discrete grasp sets by 63% on simulated Franka grasping tasks. The key contributions of the paper are:

- Neural Grasp Distance Fields (NGDF), a neural implicit function that represents grasp manifolds as a continuous level set, and predicts the distance of a query pose to the level set.
- A gradient-based optimization algorithm that incorporates NGDF for reach and grasp planning. The algorithm uses NGDF to provide grasp costs and gradients that are jointly optimized with other trajectory costs such as smoothness and collision avoidance.

II. RELATED WORK

While grasping and motion planning are well-studied topics in robotics, prior works often propose different system design decisions and operate under different assumptions, making comparison and contextualization difficult. We provide a summary of the most important design decisions for 6-DOF grasp and motion planning pipelines (see Fig. 2) and trace the decisions in some representative methods.

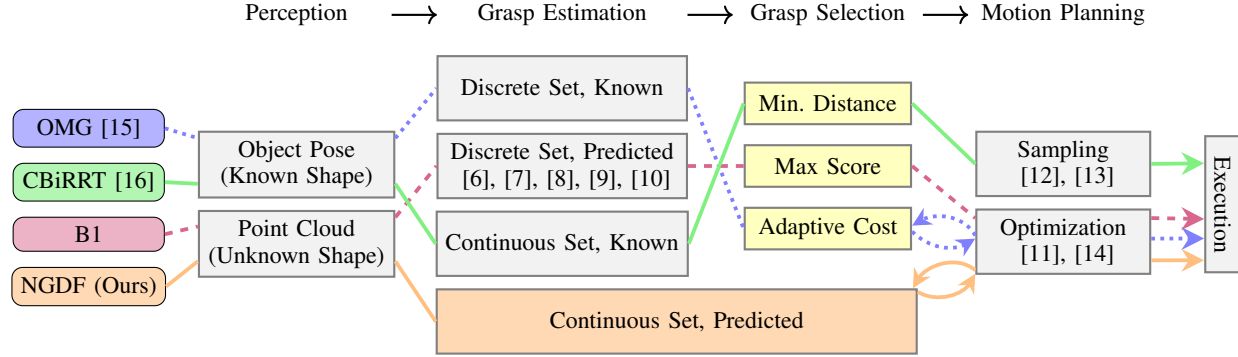


Fig. 2: Columns illustrate design decisions within grasp and motion planning pipelines. The left-most column highlights representative pipelines like **OMG-Planner** [15], **CBiRRT** [16], and baseline **B1** from Table II which uses a SOTA grasp estimator [6]. The respective design choices for these methods are traced through the columns. We identify **learned continuous representations** as an under-explored option for grasp estimation, and propose **NGDF** as a solution that does not require a heuristic **grasp selection step** since the grasp pose is jointly optimized with motion planning.

A. 6-DOF Grasp Estimation

The task of 6-DOF grasp estimation is to predict $SE(3)$ poses that are successful grasps on objects when a gripper moves to the predicted pose and closes its fingers. 6-DOF grasping is a well-studied task [17], [18]; we focus here on recent, data-driven methods. Several methods learn 6-DOF grasp estimation from point clouds [7], [6], [8], [9], [10]. Contact-GraspNet [6], a state-of-the-art method in explicit grasp estimation, predicts both grasp parameters and a grasp quality score for each local region of a point cloud scene, training on ground truth grasps where at least one of the two grasp contact points are unoccluded prior to grasping.

These methods output a discrete set of grasps and thus only represent a subset of the true continuous grasp set. Outputting a finer discretization comes with a cost of a greater computational complexity for both grasp estimation as well as grasp selection: a final grasp must be chosen from the predicted set. Because these methods only predict discrete grasp sets, they necessitate a multi-stage approach, which can be brittle if any of the stages (grasp estimation, selection, or motion planning) fails. Our approach does not have these concerns as we model grasps as the level set of a continuous implicit function, and use this function with an optimizer to jointly optimize grasping and motion planning.

B. Joint Grasp Selection and Motion Planning

We now review methods that address the task of motion planning given a set of valid grasps. Berenson et al. [16] define goal sets as a continuous range of pose transformations, or task space regions. The method samples goals in these continuous regions and uses sampling-based planning to reach the goals. Goal-set CHOMP [19] operates on discrete grasp sets, projecting the final joint configuration in a trajectory back to the goal set after an unconstrained functional gradient update. GOMP [20] uses sequential quadratic programming to optimize discrete grasp sets. OMG-Planner [15] uses online learning for grasp costs to facilitate switching between grasps in a discrete grasp set; they demonstrate their approach for known grasps, though their method can be applied to predicted grasps as well. Our

approach uses NGDF with gradient-based optimization to produce smooth, collision-free trajectories that reach a valid grasp.

Other works propose closed-loop methods for joint 6-DOF grasp and motion planning. Wang *et al.* [21] learn a latent space of trajectories for closed-loop grasping. Song *et al.* [22] learn a closed-loop policy to move the end effector towards a good grasp, but requires human demonstrations. Temporal GraspNet [23] uses importance sampling per timestep to evaluate the viability of a discrete set of grasps. In this work, we introduce a novel implicit representation that models the grasp manifold as a continuous distance function. We focus on open-loop planning with this representation and leave closed-loop planning with NGDF as future work.

C. Implicit Neural Representations

Prior work in the vision and graphics communities have achieved impressive results using implicit neural representations on novel view synthesis [1] and 3D reconstruction [3], [2]. Despite differences in tasks, these works all employ implicit functions to take a query point as input and predict the value at that point of a visual concept such as radiance [1], occupancy [3], [5], or distance to a surface [2], [4]. Methods that predict distances are particularly relevant to our work, as NGDF predicts unsigned distances between query poses and grasp poses, applying concepts from DeepSDF [2] and Neural Unsigned Distance Fields [4] to $SE(3)$ manifolds. Karunratakul *et al.* [24] learn an implicit representation for human grasp poses; we learn a representation for gripper poses and use our learned representation to optimize grasp trajectories.

The robotics community has also explored learning neural implicit functions for various tasks, such as transparent object perception [25], [26], tool deformation [27], imitation learning [28], [29], visuo-motor control [30], and to represent manipulation objectives [31]. GIGA [32] proposed using neural implicit functions to model both 3D shape and grasp quality as continuous representations. However, GIGA predicts grasp parameters along with grasp quality scores, restricting the method to output a single grasp parameterization per 3D location. GIGA also requires a sampling procedure to select

the final grasp pose from the implicit set. Our approach predicts grasp distance, allowing multiple grasp orientations per 3D location, and uses optimization to minimize grasp distance and achieve the final grasp pose.

Concurrent works have proposed learning continuous representations for dexterous grasps [33] and multiple robot hands [34]. Uraint *et al.* [35] propose representing grasps as diffusion fields, framing joint grasp and motion planning as an inverse diffusion process. In this paper, we represent grasps using implicit functions and use gradient-based trajectory optimization for joint grasp and motion planning.

III. BACKGROUND

Neural Implicit Functions. Neural implicit functions (NIFs) are neural networks that take a query $\mathbf{q} \in \mathbb{R}^d$ and optionally a context embedding $\mathbf{z} \in \mathcal{Z}$ to output a scalar value that represents a relationship to an underlying distribution: $f(\mathbf{q}, \mathbf{z}) : \mathbb{R}^d \times \mathcal{Z} \mapsto \mathbb{R}$. In the domain of 3D shape reconstruction, the context z is a latent shape embedding, the query q is a 3D point, and the scalar output is either occupancy [3], [5], or distance to the closest surface [2], [4]. The surface of the shape is represented by the zero level set in distance-based methods, or the decision boundary in occupancy-based methods. Unlike explicit functions, NIFs are not limited by resolution as they can predict a value at any query point, and they can also better represent underlying distributions that are disjoint [28]. Our approach leverages both properties in learning continuous manifold of grasps.

Gradient-based Trajectory Optimization. Trajectory optimization aims to find a trajectory $\xi \in \Xi$ that maps time to robot joint angle configurations $\xi : [0, T] \rightarrow q \in C$ by minimizing an objective functional \mathcal{U} :

$$\xi^* = \arg \min_{\xi} \mathcal{U}[\xi], \text{ s.t. } \xi(0) = q_s, \xi(T) = q_g \quad (1)$$

for a given start q_s and goal q_g configuration. In manipulation, the objective \mathcal{U} often contains cost terms for smoothness and collision avoidance. CHOMP [11] solves for ξ^* , the locally optimal solution to the non-convex objective, with functional gradient descent:

$$\xi_{t+1} = \xi_t - \eta A^{-1} \bar{\nabla} \mathcal{U}(\xi_t) \quad (2)$$

where A is an acceleration metric that helps propagate updates over the entire trajectory.

IV. METHOD

In this work, we represent a set of poses $\mathcal{M} \subset \text{SE}(3)$ as the level set of a neural implicit function. This implicit function takes a query pose \mathbf{q} as input and estimates its distance to the learned level set. In Sec. IV-A, we describe how our Neural Grasp Distance Fields (NGDF) leverages this insight to learn the level set of valid grasp poses. In Sec. IV-B, we explain how to incorporate NGDF into a trajectory optimization framework to jointly reason over smooth and collision-free reaching trajectories that end at a valid grasp pose. Fig. 3 provides an overview of our method.

A. Neural Grasp Distance Fields

Given a query pose $\mathbf{q} \in \text{SE}(3)$ and a shape embedding $\mathbf{z} \in \mathcal{Z}$, NGDF defines an implicit function:

$$\text{NGDF}(\mathbf{q}, \mathbf{z}) = \mathbf{d} \quad (3)$$

where \mathbf{d} is the distance from \mathbf{q} to the closest valid grasp $\mathbf{g} \in \mathcal{M} \subset \text{SE}(3)$ for an object in a scene. Valid grasps are poses where a gripper can stably grasp an object by closing its fingers. For the distance metric \mathbf{d} we combine translation and orientation distances into a single “control points” metric [7]:

$$d_i = \|\mathcal{T}(\mathbf{q}; \mathbf{p}_i) - \mathcal{T}(\mathbf{g}; \mathbf{p}_i)\|_1, \quad i = 0, \dots, N \quad (4)$$

where $\mathcal{T}(\cdot; \mathbf{p}_i)$ is the transformation of a predefined set of points $\{\mathbf{p}_i\}$ on the gripper. Since \mathbf{q} and \mathbf{g} belong to $\text{SE}(3)$, the distance could be defined based on the manifold geodesic distance between those poses, however we find that the control points based distance metric balances the translation and rotation costs better in practice. NGDF estimates the distance for each control point \mathbf{p}_i separately $\mathbf{d}(\mathbf{q}, \mathbf{g}) = [d_0, \dots, d_N]^T$. During training, the estimated distances $\hat{\mathbf{d}}$ are supervised with L1 loss: $\mathcal{L} = \|\hat{\mathbf{d}} - \mathbf{d}\|_1$.

B. Optimization of Grasping Trajectories using NGDF

NGDF outputs distance to closest grasp pose given a query pose. We show how NGDF can be incorporated as a goal cost function within gradient-based trajectory optimization with other costs such as smoothness and collision avoidance. This enables jointly optimizing for reaching and grasping.

In this work, we combine NGDF with CHOMP [11] (described in Sec. III), though NGDF can be used in any gradient-based trajectory optimization algorithms. Since CHOMP specifies a fixed goal q_g , we modify CHOMP to include q_g as a variable in the optimization following Dragan *et al.* [19]. We then add our grasp cost $\mathcal{F}_{\text{grasp}}$ as the variable goal cost to the objective functional \mathcal{U} :

$$\mathcal{U}[\xi] = \lambda_1 \mathcal{F}_{\text{grasp}}[\xi] + \lambda_2 \mathcal{F}_{\text{smooth}}[\xi] + \lambda_3 \mathcal{F}_{\text{obs}}[\xi] \quad (5)$$

where λ_i are cost weights.

Grasp Distance as a Goal Cost. We now define $\mathcal{F}_{\text{grasp}}$ and derive its functional gradient $\bar{\nabla} \mathcal{F}_{\text{grasp}}$ for gradient-based optimization. For a trajectory (during any iteration of optimization), we calculate the gripper pose from the final joint configuration using forward kinematics: $\mathbf{q}_T = \text{FK}(\xi_T)$. We then use NGDF to estimate the distance of this gripper pose to a valid grasp, and use this distance as our grasp cost:

$$\mathcal{F}_{\text{grasp}}[\xi] = \frac{1}{N} \sum_i^N |\hat{d}_i|, \quad \hat{\mathbf{d}} = \text{NGDF}(\mathbf{q}_T, \mathbf{X}). \quad (6)$$

We can compute the gradient of the grasp cost with respect to the joint configuration ξ_T through backpropagation:

$$\frac{\partial \mathcal{F}_{\text{grasp}}}{\partial \xi_T} = \frac{\partial \mathcal{F}_{\text{grasp}}}{\partial \theta_{\text{NGDF}}} \frac{\partial \theta_{\text{NGDF}}}{\partial \text{FK}} \frac{\partial \text{FK}}{\partial \xi_T} \quad (7)$$

where θ_{NGDF} are the neural network parameters of NGDF. Since the grasp cost only applies to the final configuration in a trajectory, the functional gradient $\bar{\nabla} \mathcal{F}_{\text{grasp}}$ contains all zeros except for the last row: $\bar{\nabla} \mathcal{F}_{\text{grasp}} = [\mathbf{0}, \mathbf{0}, \dots, \frac{\partial \mathcal{F}_{\text{grasp}}}{\partial \xi_T}]^T$.

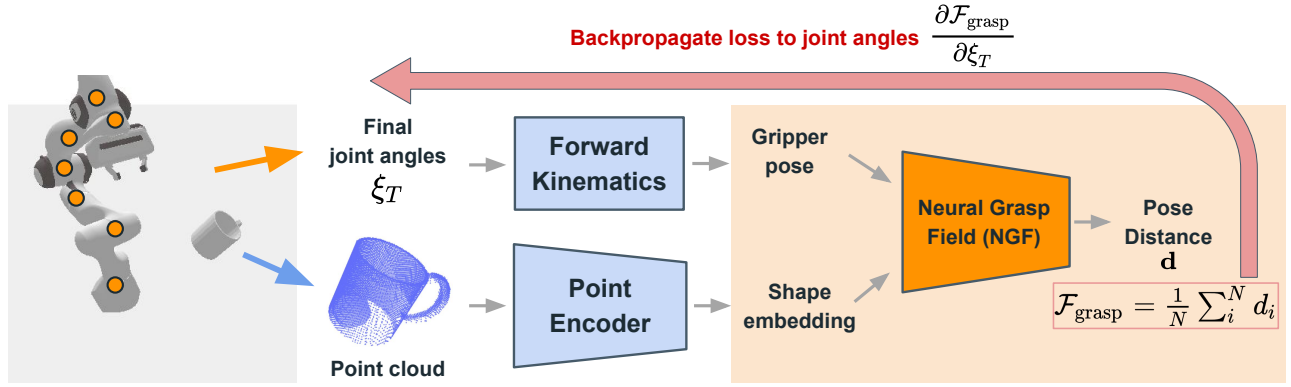


Fig. 3: We use NGDF as a goal cost function on the final state of a trajectory during gradient-based optimization. Given the current robot joint configuration and a point cloud of an object or scene, the current gripper pose and a shape embedding are computed as inputs for NGDF. Then, NGDF predicts the distance of the current gripper pose to the closest grasp (Sec. IV-A). The predicted distance is used as the cost and the gradient with respect to the joint configuration is computed with backpropagation. This cost (with gradient) is used with other costs like smoothness and collision avoidance to update the trajectory (Sec. IV-B).

Joint Optimization of Trajectory Costs. Similar to the objective functional (Eq. 5), the objective functional gradient $\bar{\nabla}\mathcal{U}$ is a weighted sum of gradients:

$$\bar{\nabla}\mathcal{U}[\xi] = \lambda_1 \bar{\nabla}\mathcal{F}_{\text{grasp}} + \lambda_2 \bar{\nabla}\mathcal{F}_{\text{smooth}} + \lambda_3 \bar{\nabla}\mathcal{F}_{\text{obs}}. \quad (8)$$

At every optimization iteration, we compute the costs and functional gradients as described above, then update the trajectory according to the A -metric update rule (Eq. 2). Since our objective cost has terms for minimizing the distance to a valid grasp, maintaining smoothness, and avoiding collisions, our algorithm can jointly optimize all three to produce successful reaching and grasping trajectories.

C. Implementation Details

Dataset. Training NGDF requires a dataset of point clouds, valid grasp poses, and query poses. We use the ACRONYM [36] dataset, which contains object meshes and successful grasp poses collected in NVIDIA FleX [37]. Point clouds are sampled from the object meshes. For grasp poses, our evaluations in Sec. V are run in PyBullet [38], so we relabel the successful grasp poses based on their success in PyBullet with the same linear and rotational shaking parameters used in ACRONYM. In addition, we filter the positive grasp set to only include grasps where the normals at the mesh and finger contact points are opposed to each other (-0.98 cosine similarity). Our results in Sec. V-B show that this filtering improves grasp performance. To collect query poses for the dataset, we sample 1 million random SE(3) poses within a 0.5 m radius of the object mesh centroid. For each sampled pose, we use distance to the closest grasp in the valid grasp set (see Sec. IV-A) as our supervision.

Architecture. An input point cloud is converted into the shape embedding \mathbf{z} using a VN-OccNet [39] encoder pre-trained on 3D reconstruction [29]. The input to NGDF is a concatenation of this shape embedding \mathbf{z} with the input query \mathbf{q} 's position and quaternion. The NGDF network is based on DeepSDF [2] and consists of 8 MLP layers, 512 units each, and ReLU activations on the hidden layers. A softplus activation on the output layer ensures positive outputs.

Training Procedure. We freeze the weights of the pre-trained point encoder during training and only train the NGDF network. During training, we sample a tuple from the dataset containing a partial point cloud, a query pose and the closest valid grasp. The partial point cloud is merged together from 4 camera views and downsampled to 1500 points using farthest point sampling. Random rotation augmentations are applied to each training sample with $p = 0.7$. Finding the ground truth closest grasp pose is computationally expensive and requires multiple simulated grasp attempts per query pose. Therefore, our supervision is pseudo-ground truth, as the closest grasp pose comes from a large but discrete set of grasps [36]. We find that this discrete grasp set is dense enough to train NGDF, while still representing unseen valid grasp poses at or near the zero level set (Sec. V-A).

Trajectory Optimization. CHOMP [11] uses a fixed or decaying step size for functional gradient updates, which is sufficient for trajectories with fixed start and goal joint configurations. However, with our modification of CHOMP in Sec. IV-B to allow a variable goal configuration, we found that such simple step size strategies resulted in poor convergence. We address this issue by using Adam [40] to adaptively update the step size (“CHOMP-Adam”). We use differentiable SE(3) operations [41] and a differentiable robot model [42] to backpropagate gradients from the output of NGDF to the robot joint configuration (Eq. 7).

V. EXPERIMENTS

We first evaluate how well the NGDF model learns to represent valid grasp manifolds as their zero level sets (Sec. V-A). Then we perform a full system evaluation of NGDF on a “reaching and grasping” task (Sec. V-B), where NGDF is used within a gradient-based trajectory optimizer as a goal cost function. Finally, we evaluate the NGDF model’s generalization on grasping intra-category unseen objects (Sec. V-C).

A. Evaluating the Grasp Level Set of NGDF

First, we investigate whether the learned level set of an NGDF represents successful grasps. Our evaluation proce-

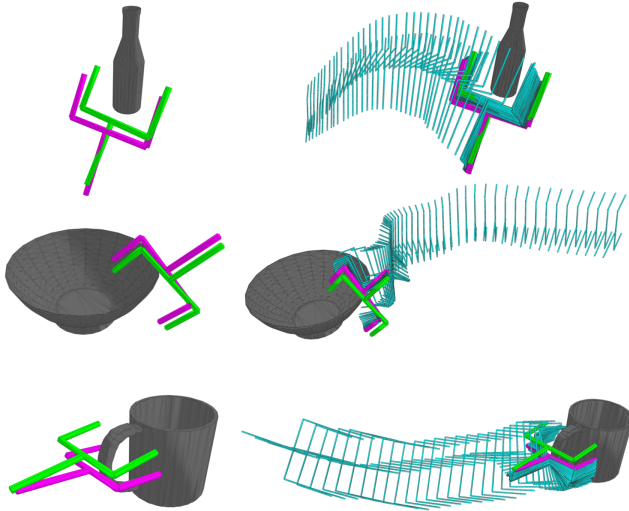


Fig. 4: Grasp level set evaluation. Left: Final predicted pose (magenta) and its closest grasp pose (green) in the training dataset. Right: Path (teal) of the gripper as it is optimized from the initial pose to the final pose. Object meshes are shown for visual clarity; our method takes point clouds as input.

TABLE I: NGDF Grasp Level Set Results

	Train Set Error \downarrow	Grasp Success \uparrow
Bottle-NoFilter	0.023 \pm 0.01	0.480 \pm 0.50
Bottle	0.029 \pm 0.01	0.880 \pm 0.32
Bowl-NoFilter	0.036 \pm 0.02	0.540 \pm 0.50
Bowl	0.033 \pm 0.01	0.760 \pm 0.43
Mug-NoFilter	0.038 \pm 0.01	0.680 \pm 0.47
Mug	0.035 \pm 0.01	0.860 \pm 0.35

Results are averaged over 50 unseen query poses per object.

ture considers driving an initial query pose to the learned level set. We use the distance output from NGDF as a loss, and update the query pose with Adam [40] using backpropagated gradients. Note that this evaluation optimizes just the gripper pose; full-arm trajectory optimization is considered in the next subsection. We evaluate NGDF on three objects: Bottle, Bowl, and Mug. For this evaluation, we train a single NGDF model for each object, and evaluate models trained with and without the dataset filtering procedure described in Sec. IV-C. We run the optimization for 3k steps with a learning rate of 1e-4. Since we represent poses as positions and quaternions, we normalize the quaternion after each gradient update to ensure valid rotations.

The quantitative results on grasp level set optimization are shown in Table I. We use two metrics for this evaluation. The “Train Set Error” metric is the minimum control points distance (Eq. 4) between the optimized gripper pose and the closest grasp pose in the discrete training set. Since NGDF should learn a continuous level set and interpolate between grasps in the training set, we expect NGDF not to achieve zero error on this metric, but it provides a good surrogate for comparing models. The “Grasp Success” metric measures the grasp quality of the optimized gripper poses. For each pose, we load the target object in PyBullet [38] and attempt a grasp

at the specified pose. The robot gripper is always initialized to the same position; the object is transformed relative to the gripper. Linear and rotational shaking are applied after gripping the object [36], and the grasp is successful if the object is still gripped after the shaking.

Our results show that while NGDFs trained on filtered and unfiltered data have similar Train Set Error, the Grasp Success for filtered data models is much higher. These results also indicate that NGDFs have learned continuous level sets, since the mean distance predicted by NGDF after optimization is less than 1e-5, much lower than the minimum distance to the training set of grasps. Qualitative results for the optimization path and final gripper pose are shown in Fig. 4.

B. Reaching and Grasping Evaluation

Next, we evaluate our method on a full reaching and grasping task, which requires planning a smooth, collision-free trajectory for the full robot arm starting from an initial robot joint configuration to grasp an object. This evaluates over a full pipeline as opposed to just the stand-alone gripper pose in the previous subsection. The task is considered successful if the robot executes the trajectory, closes its fingers to grasp the object, and lifts the object without losing it. We place Bottle, Bowl, and Mug objects in simulation in 30 random orientations each (see Fig. 5 left-most column) and thus 90 trials in total. Our results indicate that even in such a seemingly simple setting, these objects with random orientations present an overall challenging benchmark.

For this evaluation, we train a separate NGDF (similar to NeRF approaches [1], [26]) for each object, though our method can be extended to generalize across objects like other shape-conditioned implicit approaches [2]. We also evaluate intra-category (known class, unseen shape) generalization in the next subsection. We run 500 iterations of CHOMP-Adam (see Sec. IV-C) with a learning rate of 3e-3. The grasp cost is weighted heavily relative to the collision and smoothness costs. The trajectory is initialized using inverse kinematics so the gripper pose of the final joint configuration is within 0.3 m of the center of the object point cloud; the rest of the initial trajectory is interpolated between the start and end joint configurations.

The results are shown in Table II. We compare against oracle methods that provide upper-bound task performance, and against baselines that predict discrete grasps. The oracle methods assume perfect object pose estimation and known discrete grasp set. All discrete grasp methods run inverse kinematics over all discrete grasp goals and discard infeasible grasps before planning. “O1” selects the goal with minimum distance to the initial joint configuration, and keeps it fixed throughout planning (Fixed Goal). “OMG” [15] adaptively learns a cost for each grasp and selects the grasp with minimum cost at every optimization iteration (Variable Goal).

The baselines that predict discrete grasps use Contact-Grasnet [6] as the grasp estimator. We use weights (provided by the authors) that are trained on millions of grasps and shapes. “B1” selects the grasp goal with the maximum

TABLE II: Reaching and Grasping Results

Method	Perception	Grasp Estimation	Grasp Selection	Goal	Execution Success \uparrow
O1 (Oracle)	Known Object Pose	Known Discrete Grasps	Min. Distance	Fixed	0.96 \pm 0.2
OMG [15] (Oracle)	Known Object Pose	Known Discrete Grasps	Adaptive Cost	Variable	0.99 \pm 0.1
B1	Unknown Object Pose	Predicted Discrete Grasps [6]	Max Score	Fixed	0.37 \pm 0.5
B2	Unknown Object Pose	Predicted Discrete Grasps [6]	Min. Distance	Fixed	0.39 \pm 0.5
B3	Unknown Object Pose	Predicted Discrete Grasps [6]	Min. Distance	Variable	0.38 \pm 0.5
B4	Unknown Object Pose	Predicted Discrete Grasps [6]	Adaptive Cost	Variable	0.31 \pm 0.5
NGDF (Ours)	Unknown Object Pose	Predicted Continuous Grasps	N/A	Variable	0.61 \pm 0.5

Middle columns correspond to design decisions found in Fig. 2; color-coded methods also correspond to those shown in the same figure.

score estimated by Contact-GraspNet and keeps it fixed during planning. “B2” selects the grasp goal with minimum distance to the initial joints and keeps it fixed during planning. “B3” allows varying grasps during planning using the minimum distance metric. “B4” uses the same adaptive cost from OMG [6] to select grasp goals during planning.

Our results show that while the oracle methods using known object poses and known grasps perform well, methods that don’t assume known object pose and use predicted grasps have much lower Execution Success. Of the predicted grasp methods, NGDF performs best. Surprisingly, the B3 and B4 variable goal variants do not outperform fixed goal variants B1 and B2. Failure cases for all methods are largely due to collisions between the gripper fingers and the object, which are a relatively small obstacle cost and may be difficult for the planner to balance with the other costs. Qualitative results for NGDF are shown in Fig. 5.

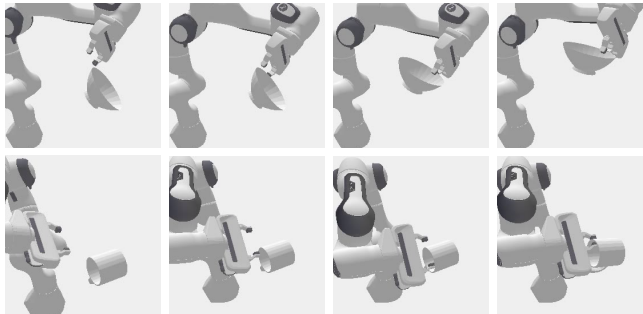


Fig. 5: Successful grasp trajectories (left-to-right) planned by our method for the bowl (top) and mug (bottom). Additional examples and media are available on the [project page](#).

C. Intra-Category Generalization

To evaluate whether our method can generalize to shapes in the same object category, we train an NGDF model on 7 shapes in the “Bottle” category from ACRONYM [36]. Training samples are generated from the meshes using the same data collection procedure described in Sec. IV-C. We evaluate performance on a held-out Bottle instance, the same instance used in the previous evaluations. The intra-category model achieves 0.63 ± 0.5 execution success on 30 Bottle trials for the reaching and grasping evaluation, which is comparable with the single-object NGDF results from Table II, demonstrating intra-category generalization without loss of performance.

VI. DISCUSSION

Neural implicit functions have been widely explored for 3D vision tasks such as shape reconstruction. NGDF extends this concept to grasp estimation, using 6D poses as queries on continuous grasp manifolds. Our work differs from existing work on 3D reconstruction, not only due to the higher dimensionality of our problem, but also because of the challenge in acquiring ground truth labels. The ground truth grasp distance between an arbitrary query pose and the corresponding closest grasp is expensive to compute in simulation. Instead, we train on large-scale discrete grasp sets [36] as near-ground truth supervision. Our experiments in Sec. V-A show that NGDF is able to learn the grasp level set from this supervision, and interpolate between the discrete grasps to represent the continuous grasp manifold.

NGDF decouples the problem of learning a representation of the grasp manifold from the problem of finding a good grasp pose. To solve the latter, we formulate the distance output of NGDF as a cost to be minimized. For the full robot motion planning regime, we use a trajectory optimization algorithm to optimize the grasp cost jointly with other trajectory costs such as smoothness and collision avoidance. We outperform several baselines in Sec. V-B that represent what a practitioner would implement for a reaching and grasping task. While the performance of oracle methods indicate room for improvement, our results show that joint optimization with NGDF is a promising direction for manipulation. We also demonstrate the scalability of our approach with intra-category generalization results in Sec. V-C.

In terms of limitations, NGDF is trained on a gripper-specific dataset; NGDF for other grippers will likely require different datasets. Further, optimizing cost weights are fixed for the joint optimization in the reach and grasp planning task; estimating the cost weights per optimization iteration could improve performance.

VII. CONCLUSION

We propose Neural Grasp Distance Fields (NGDF), which represents the continuous manifold of grasps as zero-level set of a neural field. We formulate the estimated distance as a cost for a gradient-based trajectory optimizer to jointly optimize with other trajectory costs such as smoothness and collision avoidance to perform reach and grasp planning. Our results show that NGDF outperforms existing methods, while generalizing to unseen poses and unseen objects.

ACKNOWLEDGMENT

The authors thank Kalyan Alwala and Adithya Murali for early discussions and prototyping of this work. We thank Daniel Seita and Chuer Pan for feedback on the paper draft.

APPENDIX

A. Ablations for Neural Grasp Distance Fields

We perform ablation experiments for our trajectory optimizer (Table S1). We compare using Adam [40] vs. a fixed step size (“No-Adam”) for functional gradient descent. Unlike our method, CHOMP [11] originally uses a fixed or decaying step size, in the setting where the start and end trajectory configurations are not optimized (Sec. IV-B). In our setting, the end configuration is variable to allow optimization of the grasp pose. No-Adam converges slowly when the trajectory is far from a valid grasp pose, and overshoots when near the level set. We also evaluated using a decaying step size; while this mitigated the overshooting issue, convergence was still much slower, and the decay rate required tuning.

“No-Initial-IK” initializes the configuration at every timestep in the trajectory to the starting joint configuration, instead of using IK to initialize the trajectory as described in Sec. V-B. We observe worse performance with No-Initial-IK as the initial trajectory is farther from the desired grasp trajectory, making it harder to plan.

TABLE S1: Optimizer Ablation Results

Grasp Execution \uparrow	
NGDF, No-Adam	0.18 ± 0.4
NGDF, No-Initial-IK	0.44 ± 0.5
NGDF (Ours)	0.61 ± 0.5

No-Adam uses CHOMP [11] with a fixed step size instead of Adam [40] optimization for the functional gradient update. No-Initial-IK initializes the trajectory so all steps in the plan start at the initial joint configuration. NGDF uses Adam and initializes the endpoint of the trajectory using inverse kinematics to achieve the best performance.

REFERENCES

- [1] B. Mildenhall, P. P. Srinivasan, M. Tancik, J. T. Barron, R. Ramamoorthi, and R. Ng, “Nerf: Representing scenes as neural radiance fields for view synthesis,” in *ECCV*, 2020.
- [2] J. J. Park, P. Florence, J. Straub, R. Newcombe, and S. Lovegrove, “Deepsdf: Learning continuous signed distance functions for shape representation,” in *Proceedings of the IEEE/CVF Conference on Computer Vision and Pattern Recognition*, 2019, pp. 165–174.
- [3] L. Mescheder, M. Oechsle, M. Niemeyer, S. Nowozin, and A. Geiger, “Occupancy networks: Learning 3d reconstruction in function space,” in *Proceedings of the IEEE/CVF Conference on Computer Vision and Pattern Recognition*, 2019, pp. 4460–4470.
- [4] J. Chibane, A. Mir, and G. Pons-Moll, “Neural unsigned distance fields for implicit function learning,” in *Advances in Neural Information Processing Systems (NeurIPS)*, December 2020.
- [5] J. Chibane, T. Alldieck, and G. Pons-Moll, “Implicit functions in feature space for 3d shape reconstruction and completion,” in *IEEE Conference on Computer Vision and Pattern Recognition (CVPR)*. IEEE, jun 2020.
- [6] M. Sundermeyer, A. Mousavian, R. Triebel, and F. Dieter, “Contact-grasnet: Efficient 6-dof grasp generation in cluttered scenes,” *IEEE International Conference on Robotics and Automation (ICRA)*, 2021.
- [7] A. Mousavian, C. Eppner, and D. Fox, “6-dof grasnet: Variational grasp generation for object manipulation,” in *Proceedings of the IEEE/CVF International Conference on Computer Vision*, 2019, pp. 2901–2910.
- [8] P. Ni, W. Zhang, X. Zhu, and Q. Cao, “Pointnet++ grasping: Learning an end-to-end spatial grasp generation algorithm from sparse point clouds,” in *2020 IEEE International Conference on Robotics and Automation (ICRA)*, 2020, pp. 3619–3625.
- [9] H. Liang, X. Ma, S. Li, M. Görner, S. Tang, B. Fang, F. Sun, and J. Zhang, “Pointnetgpd: Detecting grasp configurations from point sets,” in *2019 International Conference on Robotics and Automation (ICRA)*. IEEE, 2019, pp. 3629–3635.
- [10] H.-S. Fang, C. Wang, M. Gou, and C. Lu, “Grasnet-1billion: A large-scale benchmark for general object grasping,” in *Proceedings of the IEEE/CVF Conference on Computer Vision and Pattern Recognition (CVPR)*, 2020, pp. 11444–11453.
- [11] M. Zucker, N. Ratliff, A. D. Dragan, M. Pivtoraiko, M. Klingensmith, C. M. Dillin, J. A. Bagnell, and S. S. Srinivasa, “Chomp: Covariant hamiltonian optimization for motion planning,” *The International Journal of Robotics Research*, vol. 32, no. 9-10, pp. 1164–1193, 2013.
- [12] J. Kuffner and S. LaValle, “Rrt-connect: An efficient approach to single-query path planning,” in *Proceedings 2000 ICRA. Millennium Conference. IEEE International Conference on Robotics and Automation. Symposia Proceedings (Cat. No.00CH37065)*, vol. 2, 2000, pp. 995–1001 vol.2.
- [13] L. Kavraki, P. Svestka, J.-C. Latombe, and M. Overmars, “Probabilistic roadmaps for path planning in high-dimensional configuration spaces,” *IEEE Transactions on Robotics and Automation*, vol. 12, no. 4, pp. 566–580, 1996.
- [14] M. Mukadam, J. Dong, X. Yan, F. Dellaert, and B. Boots, “Continuous-time gaussian process motion planning via probabilistic inference,” *The International Journal of Robotics Research*, vol. 37, no. 11, pp. 1319–1340, 2018.
- [15] L. Wang, Y. Xiang, and D. Fox, “Manipulation trajectory optimization with online grasp synthesis and selection,” in *Robotics: Science and Systems (RSS)*, 2020.
- [16] D. Berenson, S. Srinivasa, and J. Kuffner, “Task space regions: A framework for pose-constrained manipulation planning,” *The International Journal of Robotics Research*, vol. 30, no. 12, pp. 1435–1460, 2011.
- [17] J. Bohg, A. Morales, T. Asfour, and D. Kragic, “Data-driven grasp synthesis—a survey,” *IEEE Transactions on Robotics*, vol. 30, no. 2, pp. 289–309, 2014.
- [18] K. Kleeberger, R. Bormann, W. Kraus, and M. F. Huber, “A survey on learning-based robotic grasping,” *Current Robotics Reports*, vol. 1, no. 4, pp. 239–249, 2020.
- [19] A. D. Dragan, N. D. Ratliff, and S. S. Srinivasa, “Manipulation planning with goal sets using constrained trajectory optimization,” in *2011 IEEE International Conference on Robotics and Automation*, 2011, pp. 4582–4588.
- [20] J. Ichnowski, M. Danielczuk, J. Xu, V. Satish, and K. Goldberg, “Gomp: Grasp-optimized motion planning for bin picking,” in *2020 IEEE International Conference on Robotics and Automation (ICRA)*. IEEE, 2020, pp. 5270–5277.
- [21] L. Wang, Y. Xiang, W. Yang, A. Mousavian, and D. Fox, “Goal-auxiliary actor-critic for 6d robotic grasping with point clouds,” in *Proceedings of the 5th Conference on Robot Learning*, ser. Proceedings of Machine Learning Research, A. Faust, D. Hsu, and G. Neumann, Eds., vol. 164. PMLR, 08–11 Nov 2022, pp. 70–80. [Online]. Available: <https://proceedings.mlr.press/v164/wang22a.html>
- [22] S. Song, A. Zeng, J. Lee, and T. Funkhouser, “Grasping in the wild: Learning 6dof closed-loop grasping from low-cost demonstrations,” *IEEE Robotics and Automation Letters*, vol. 5, no. 3, pp. 4978–4985, 2020.
- [23] W. Yang, C. Paxton, A. Mousavian, Y.-W. Chao, M. Cakmak, and D. Fox, “Reactive human-to-robot handovers of arbitrary objects,” *IEEE International Conference on Robotics and Automation (ICRA)*, 2021.
- [24] K. Karunratanakul, J. Yang, Y. Zhang, M. J. Black, K. Muandet, and S. Tang, “Grasping field: Learning implicit representations for human grasps,” in *2020 International Conference on 3D Vision (3DV)*. IEEE, 2020, pp. 333–344.

[25] L. Zhu, A. Mousavian, Y. Xiang, H. Mazhar, J. van Eenbergen, S. Debnath, and D. Fox, “Rgb-d local implicit function for depth completion of transparent objects,” in *Proceedings of the IEEE/CVF Conference on Computer Vision and Pattern Recognition*, 2021, pp. 4649–4658.

[26] J. Ichniowski*, Y. Avigal*, J. Kerr, and K. Goldberg, “Dex-NeRF: Using a neural radiance field to grasp transparent objects,” in *Conference on Robot Learning (CoRL)*, 2020.

[27] Y. Wi, P. Florence, A. Zeng, and N. Fazeli, “Virdo: Visio-tactile implicit representations of deformable objects,” 2022.

[28] P. Florence, C. Lynch, A. Zeng, O. A. Ramirez, A. Wahid, L. Downs, A. Wong, J. Lee, I. Mordatch, and J. Tompson, “Implicit behavioral cloning,” in *Conference on Robot Learning*. PMLR, 2022, pp. 158–168.

[29] A. Simeonov, Y. Du, A. Tagliasacchi, J. B. Tenenbaum, A. Rodriguez, P. Agrawal, and V. Sitzmann, “Neural descriptor fields: Se(3)-equivariant object representations for manipulation,” *arXiv preprint arXiv:2112.05124*, 2021.

[30] Y. Li, S. Li, V. Sitzmann, P. Agrawal, and A. Torralba, “3d neural scene representations for visuomotor control,” in *Conference on Robot Learning*. PMLR, 2022, pp. 112–123.

[31] D. Driess, J.-S. Ha, M. Toussaint, and R. Tedrake, “Learning models as functionals of signed-distance fields for manipulation planning,” in *Conference on Robot Learning*. PMLR, 2022, pp. 245–255.

[32] Z. Jiang, Y. Zhu, M. Svetlik, K. Fang, and Y. Zhu, “Synergies between affordance and geometry: 6-dof grasp detection via implicit representations,” 2021.

[33] Y.-H. Wu, J. Wang, and X. Wang, “Learning generalizable dexterous manipulation from human grasp affordance,” *Conference on Robot Learning*, 2022.

[34] N. Khargonkar, N. Song, Z. Xu, B. Prabhakaran, and Y. Xiang, “Neuralgrasps: Learning implicit representations for grasps of multiple robotic hands,” *Conference on Robot Learning*, 2022.

[35] J. Uraín, N. Funk, G. Chalvatzaki, and J. Peters, “Se (3)-diffusionfields: Learning cost functions for joint grasp and motion optimization through diffusion,” *arXiv preprint arXiv:2209.03855*, 2022.

[36] C. Eppner, A. Mousavian, and D. Fox, “ACRONYM: A large-scale grasp dataset based on simulation,” in *IEEE International Conference on Robotics and Automation (ICRA)*, 2021.

[37] M. Macklin, M. Müller, N. Chentanez, and T.-Y. Kim, “Unified particle physics for real-time applications,” *ACM Trans. Graph.*, vol. 33, no. 4, jul 2014. [Online]. Available: <https://doi.org/10.1145/2601097.2601152>

[38] E. Coumans and Y. Bai, “Pybullet, a python module for physics simulation for games, robotics and machine learning,” <http://pybullet.org>, 2016–2021.

[39] C. Deng, O. Litany, Y. Duan, A. Poulenard, A. Tagliasacchi, and L. J. Guibas, “Vector neurons: A general framework for so (3)-equivariant networks,” in *Proceedings of the IEEE/CVF International Conference on Computer Vision*, 2021, pp. 12 200–12 209.

[40] D. P. Kingma and J. Ba, “Adam: A method for stochastic optimization,” *CoRR*, vol. abs/1412.6980, 2015.

[41] L. Pineda, T. Fan, M. Monge, S. Venkataraman, P. Sodhi, R. Chen, J. Ortiz, D. DeTone, A. Wang, S. Anderson *et al.*, “Theseus: A library for differentiable nonlinear optimization,” *arXiv preprint arXiv:2207.09442*, 2022.

[42] G. Sutanto, A. Wang, Y. Lin, M. Mukadam, G. Sukhatme, A. Rai, and F. Meier, “Encoding physical constraints in differentiable newton-euler algorithm,” ser. *Proceedings of Machine Learning Research*, A. M. Bayen, A. Jadbabaie, G. Pappas, P. A. Parrilo, B. Recht, C. Tomlin, and M. Zeilinger, Eds., vol. 120. The Cloud: PMLR, 10–11 Jun 2020, pp. 804–813. [Online]. Available: <http://proceedings.mlr.press/v120/sutanto20a.html>